Nanocellulose recovery from domestic wastewater

Espíndola, Suellen Pereira; Pronk, Mario; Zlopasa, Jure; Picken, Stephen J.; van Loosdrecht, Mark C.M.

DOI
10.1016/j.jclepro.2020.124507

Publication date
2021

Document Version
Final published version

Published in
Journal of Cleaner Production

Journal of Cleaner Production 280 (2021) 124507

Contents lists available at ScienceDirect

Journal of Cleaner Production

journal homepage: www.elsevier.com/locate/jclepro

Nanocellulose recovery from domestic wastewater

Suellen Pereira Espíndola [a, *], Mario Pronk [b], Jure Zlopasa [b], Stephen J. Picken [a], Mark C.M. van Loosdrecht [b]

[a] Department of Chemical Engineering, Delft University of Technology, Van der Maasweg 9, 2629 HZ, Delft, the Netherlands
[b] Department of Biotechnology, Delft University of Technology, Van der Maasweg 9, 2629 HZ, Delft, the Netherlands

ARTICLE INFO

Article history:
Received 1 June 2020
Received in revised form
29 September 2020
Accepted 30 September 2020
Available online 3 October 2020

Handling editor: Cecilia Maria Villas Bôas de Almeida

Keywords:
Cellulose
Toilet paper
Wastewater solids
Nanocellulose
Cellulose NanoCrystals
Resource recovery

ABSTRACT

Wastewater solids could be an attractive source of secondary raw cellulose, mainly originating from toilet paper. Cellulose can be recovered through sieving of raw wastewater, return sludge, or excess sludge. In particular, a large fraction of cellulose (13–15%) can be found in the excess sludge of the aerobic granular sludge produced by the Nereda® wastewater technology. A cellulose extraction method was developed during this study, allowing the recovery of a pulp with over 86 wt% purity. The wastewater derived cellulose fibres could be an excellent source for production of recovered cellulose nanocrystals (rCNC). Several pre-treatment steps needed in cellulose nanocrystals (CNC) production from wood pulp are already performed in the production of toilet paper. Here, the technical feasibility of such rCNC is studied. As reference materials, microcrystalline cellulose and toilet paper were also used. The rCNC were obtained by acid hydrolysis, with yields of ~30 wt% (pulp basis). The wastewater-based material was rod-like, with high aspect ratio (10–14), crystallinity (62–68%), and chemical structure similar to commercial CNC. The yield of rCNC per gram of cellulose recovered from the influent was 22%, while for excess sludge cellulose it was less (4%). Bio-nanocomposites of rCNC and alginate were also investigated. At 50 vol% loading of rCNC, there was a 50% relative increase in stiffness (18 GPa) compared to matrix (12 GPa). The characterization of rCNC and positive impact in composite materials confirms a suitable quality of wastewater derived CNC. Ultimately, the nanocellulose is a tangible example that recovery of high-end products from wastewater is possible, in line with a circular economy.

1. Introduction

For thousands of years, mankind process cellulose derived from plants in the production of pulp, paper, and derivatives. With the adoption of toilet paper in modern societies, cellulose fibres became, in many countries, a primary insoluble substrate entering sewage treatment plants (STP). They now compose 30–50% of the total solids in the sewage of western countries (Ghasimi et al., 2015a). A large fraction of this cellulosic matter is recalcitrant to current physicochemical and biological treatment technologies, resulting in extra surplus sludge production. Hence, more chemicals, aeration, and post-treatments are required to dispose of this urban waste. Although limited research has been conducted on the fate and recovery of cellulose in wastewaters (Chen et al., 2017; Ghasimi et al., 2016; Shun'ichi et al., 2002), the topic has lately gained the attention of water authorities.

Fine sieves have been proposed as alternative for primary clarifiers (Rusten and Odegaard, 2006), when applied at a higher loading rate mainly the cellulosic fraction is recovered from the wastewater (Ruiken et al., 2013). Recovery of the cellulosic fraction can contribute to a more circular economy and improvement of the wastewater treatment process as a whole (Reijken et al., 2018). In the last decade, a few sites have adopted this technology, mainly in Europe and North America (Nussbaum et al., 2014; Paulsrud et al., 2014; Ruiken et al., 2013; Rusten and Odegaard, 2006). Fine sieving before the biological treatment results in a fibrous mass of influent solids, which contains around 70 wt% cellulose (Fig. 1) (Ruiken et al., 2013). Due to the low biodegradability of cellulose, other common wastewater solids have a high cellulose content, such as primary and waste sludge (Shun'ichi et al., 2002). Interesting new opportunities could be opened by the widely deployed aerobic granular sludge technologies, like the Nereda® technology

Abbreviations: CNC, Cellulose NanoCrystals; rCNC, recovered Cellulose NanoCrystals; STP, Sewage Treatment Plant; TP, recycled pulp Toilet Paper.

* Corresponding author. Van der Maasweg 9, Building 58, Delft, 2629 HZ, the Netherlands.
E-mail address: S.PereiraEspindola-1@tudelft.nl (S.P. Espíndola).

https://doi.org/10.1016/j.jclepro.2020.124507

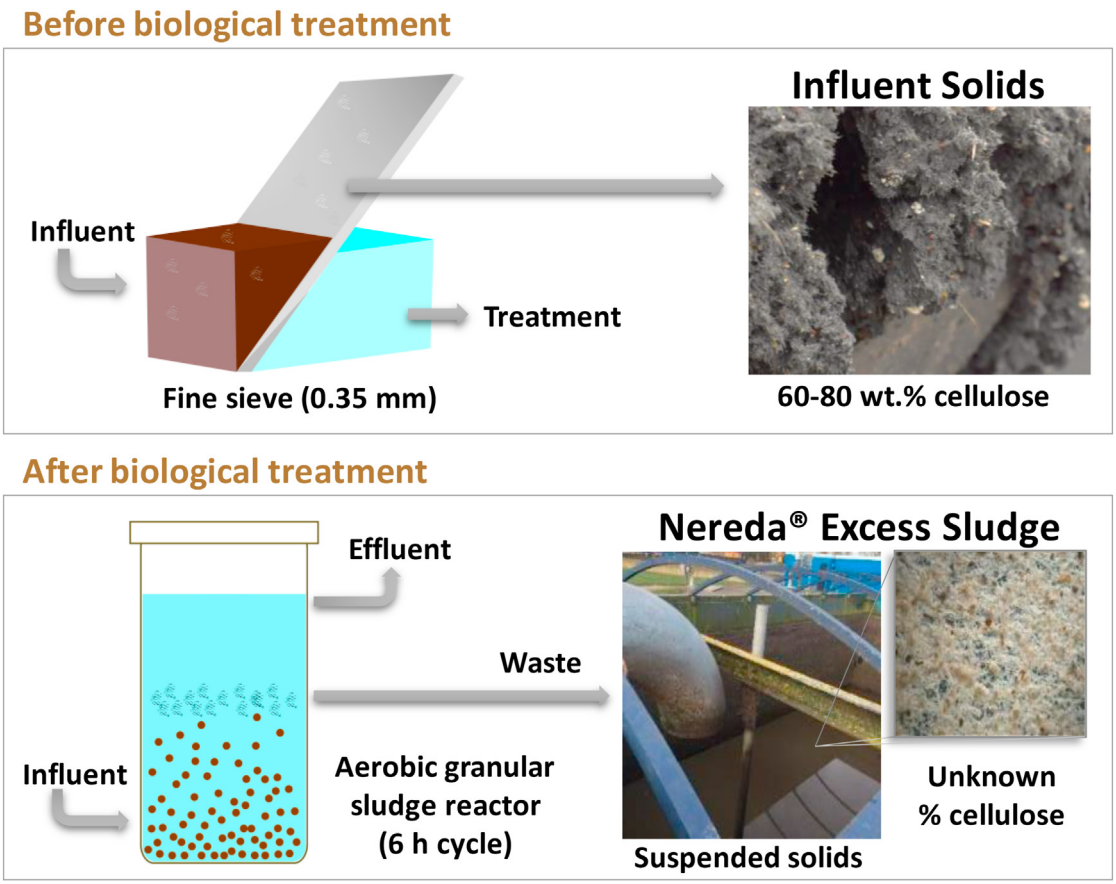

Fig. 1. The generation of cellulosic wastewater solids before and after biological treatment. The upper scheme shows the (sieved) influent solids being harvested, with 20–30 wt % total solids, of which around 60–80 wt% is cellulose. The lower scheme indicates that the suspended sludge and solids, or excess sludge, produced at the end of an aerobic granular sludge treatment cycle (around 6 h), are potentially rich in cellulose fibres.

(Pronk et al., 2015). The suspended sludge fraction (containing the influent cellulose) has a low retention time in the granular reactors (Ali et al., 2019). Thus, resulting in a relative low biodegradation of the cellulose, which accumulates in the excess sludge (Fig. 1) (Pronk, 2016).

The development of materials from wastewater can improve the economy of the water sector and integrate it in the circular economy (Leeuwen, 2018). Cellulose is a well-known renewable constituent in the production of green materials. There are many possible valorisation routes for raw cellulose. Applications can be developed using the fibre itself - in the paper, construction, furniture, textile, and automotive industries; or producing valuable chemicals, such as bioethanol and bioplastics (Ghasimi et al., 2016; Zhou et al., 2019). An interesting application could be the conversion of the wastewater derived cellulose pulp into nanocellulose.

The cellulose fibre exhibits highly ordered crystalline domains separated by less ordered domains, called amorphous regions. There are two main routes for production of the nanocrystalline cellulose: (i) mechanically, to produce Cellulose NanoFibres, and (ii) chemically, to produce Cellulose NanoCrystals (CNC). These nanocellulose fibres are potentially interesting, due to their exceptional stiffness (on par with Kevlar®), high aspect ratio, low density, low thermal expansion, simple surface modification, and low toxicity. (Börjesson and Westman, 2015; Klemm et al., 2011; Rajinipriya et al., 2018). Such properties, together with renewability and biodegradability, make nanocellulose an ideal sustainable material. There are numerous high-end applications of CNC in the composite, paper, filtration and separation, food, biomedical, automotive, and cosmetic industries (Charreau et al., 2020; Qin et al., 2020; Rajinipriya et al., 2018; Roy et al., 2018; Trache et al., 2020).

Nanocellulose as new bio-based material has gained momentum, and its production is now beyond scientific curiosity with a growing interest in research and development. Large-scale commercialization is already a reality, and there is increasing industrial interest (Mabrouk et al., 2020; Reid et al., 2017). During the past decade, the production of cellulose nanoparticles from lignocellulosic biomass, bacterial cellulose, paper and pulp industrial wastes have been extensively published (García et al., 2016; Jordan et al., 2019; Kumar et al., 2020; Rajinipriya et al., 2018; Reid et al., 2017). The potential of municipal solid waste paper for nanocellulose isolation has been recently mentioned (Hietala et al., 2018). However, the production of cellulosic nanomaterial from recovered toilet paper or wastewater solids has not been reported.

Cellulose from wastewater may be an interesting source of fibres for CNC production in comparison with the often-studied wood pulp or agricultural wastes, as several bleaching and purification steps can be avoided. These treatments have been performed in the production of the original cellulose toilet paper. Thus, recovered cellulose nanocrystals (rCNC) are explored as a new bio-based material for the valorisation of wastewater-based cellulosic material. The main goal of this study was to investigate the lab-scale production of rCNC from wastewater solids of Dutch treatment plants. The yield and the physical properties of rCNC were evaluated. Finally, bio-nanocomposites with rCNC and alginate polymer were manufactured. This had a two-fold purpose: (i) measuring the stiffness of commercial and lab-made rCNC for quality comparison

and (ii) as a material concept that may be suitable for application.

2. Material and methods

2.1. Sampling of wastewater solids

Samples were collected either through sieving of raw wastewater (section 2.1.1) or from the excess sludge of aerobic granule reactor (section 2.1.2).

2.1.1. Sieved influent solids

Screened wastewater (mesh size 6 mm) was finely sieved by a rotating belt filter equipped with a <0.35 mm pore size sieve (Salsnes Filter, Norway) at the STP Blaricum, the Netherlands, operated by Waternet. Plant size was of 30,000 p.e. and maximum hydraulic capacity 1600 m^3 h^{-1}. The retained influent solids were collected in December 2016 and stored at 4 °C before analysis. The influent solids were mainly composed of toilet paper fibres and residual sand, hair, leaves, and undefined materials. When dried, the material resembles papier-mâché. The total solids content was 162 ± 8 g kg^{-1}, with 150 ± 9 g kg^{-1} volatile, measured according to standard methods (APHA, 1998). Further information on fine sieving can be found in previous reports (Ghasimi et al., 2016; Ruiken et al., 2013).

2.1.2. Nereda® excess sludge

Excess sludge samples were taken from a Nereda® plant operated on domestic wastewater by Royal HaskoningDHV in Utrecht, the Netherlands. The Nereda® aerobic granule reactor is operated in sequencing batch mode, with process cycles of ±6 h. Within these hours, approximately 1 h is for anaerobic feeding in upwards plug-flow with simultaneous effluent withdrawal. The majority of remaining time is for aeration, followed by past settling (Giesen et al., 2013; Pronk et al., 2015). The prototype was in the start-up phase since December 19, 2016. Starting-up means the biomass concentration and granulation grade in the reactor are increasing over time. During the first sampling, cellulose fibres seemed to be building up in the reactor. The plant had a maximum hydraulic capacity of 125 m^3h^{-1} and volume of 1000 m^3. The reactor was fed with screened (6 mm) municipal wastewater. Sampling campaigns happened in January (sample NES 1) and March 2017 (sample NES 2), at the sludge buffer tank where this material is often discharged (Fig. 1). The samples were concentrated on-site by settling and decanting off clear supernatant and further stored at 4 °C. Total suspended solids (TSS) and volatile suspended solids (VSS) were measured according to standard methods (APHA, 1998). For NES 1, TSS was 13.0 ± 0.2 g L^{-1} and VSS was 11.7 ± 0.4 g L^{-1}. For NES 2, TSS was 14.0 ± 0.1 g L^{-1} and VSS was 12.5 ± 0.3 g L^{-1}. The used excess sludge was a mixture of flocculent solids that remain on the surface of the granular sludge blanket after aeration, at times combined with some granular sludge that is less frequently removed. Granules larger than 0.2 mm were mostly absent; but on the other hand, samples visibly contained seeds, sands, plastics, among other debris. For completeness, several excess sludge samples were also collected from full-scale Nereda® treatment plants across the Netherlands. The history and analysis of these samples can be found at **Text S1**, Supporting Information.

2.2. Cellulose extraction

A cellulose extracting method was developed based on a pulping process (blending and sieving in combination with the removal of water and alkaline-soluble compounds) and final bleaching treatment. The protocol is described in detail in **Text S2**, Supporting Information.

2.2.1. Extraction scheme

The standard cellulose extraction procedure is briefly described. The sample was dried, cut into 1 × 1 cm pieces and blended with demi water until forming a homogeneous suspension. It was then heated on a hot plate to 50 °C while stirring for removing water-soluble compounds. Next, the residue of filtration was placed in a beaker with an alkaline solution and heated to 80 °C. The mixture was sieved and washed thoroughly with demi water for removing alkaline-extracted compounds. This alkaline step was performed at least twice. Finally, the remaining residue was bleached with a $NaClO_2$ solution with a slightly acidic buffer. After a final sieving and washing step (until neutral pH), the resultant pulp was thoroughly dried at 60 °C. The yield of cellulose pulp was calculated based on the sample's initial solid content. All reagents were of analytical grade and used without further processing.

2.2.2. Alkaline and bleaching tests

Influent solids and excess sludge cellulose extractions were tested using a 2 wt% NaOH solution for alkalisation. Further, an extended alkaline treatment was tested for sludge due to its expected high microbial and polymeric content. Bleaching tests were performed by using a solution composed of equal parts of 1.7 wt% $NaClO_2$ and acetate buffer (27 g NaOH and 75 mL glacial acetic acid in 1 L, pH 4.6). The minimum reaction time for each bleaching step was ~6 h in a heating environment of 60–70 °C. More than one bleaching step was sometimes tested to ensure the samples were almost free of (coloured) impurities.

2.2.3. Van Soest analysis

The method of Van Soest and Wine (1967), initially developed for estimating dietary fibre fractions, was used to obtain fractions of lignin, hemicellulose, and cellulose in samples. The method is based on the combined activity of detergents. With the assay, three fibre residues were obtained: neutral detergent fibre (NDF), acid detergent fibre (ADF) and acid detergent lignin (ADL), from which it is possible to evaluate the lignin (ADL), celluloses (ADF–ADL) and hemicelluloses (NDF–ADF). The technique was applied to cellulosic pulp extracted from both influent solids and excess sludge to check for the validity of the extraction method. Recycled pulp toilet paper (TP, sampled from the university's lavatory) was also tested.

2.3. Nanocellulose (CNC) isolation

After obtaining the recovered pulp, a controlled acid hydrolysis was tested for nanocellulose isolation.

2.3.1. Materials

Sulphuric acid 95–98% was purchased from Sigma-Aldrich. For dialysis, cellulose acetate bags with 3500 Da molecular weight cut off were purchased. Avicel PH101 Eur. microcrystalline cellulose was acquired from Sigma-Aldrich. TP was first cleaned by the cellulosic pulp extraction method (section 2.2.1). A commercial sample, CelluForce® NCC, was obtained via a donation from a current industrial producer (CelluForce, Montreal, Canada). CelluForce uses 64 wt% sulphuric acid hydrolysis to produce CNC from bleached Kraft pulp. Following hydrolysis, this commercial CNC is commonly diluted, separated from residual acid, neutralised to sodium form, and spray dried. All chemicals were of analytical grade and used as received.

2.3.2. Isolation procedure

The (r)CNC isolation was initially tested via controlled acid hydrolysis with sulphuric acid (64 wt% H_2SO_4, 1:20 cellulose to acid ratio) at 45 °C. These conditions are commonly applied to paper and lignocellulosic sources (Rajinipriya et al., 2018). Following

hydrolysis, quenching, centrifugation with demi water, glass fibre vacuum filtration, neutralisation with NaOH, dialysis (4 days) and ultrasonication steps were sometimes performed. The exact hydrolysis conditions had to be modified for each cellulose source and are described in detail in **Text S3**, Supporting Information. The yield of isolated (r)CNC from the treated cellulose sources was determined gravimetrically by freeze-drying after ultrasonication.

2.3.3. Cellulose sources

Several sources were tested for CNC isolation. As reference materials, microcrystalline cellulose and TP were used first to obtain a baseline method. Then, influent solids and excess sludge pulp were tested for rCNC production. The recovered pulp was milled (mesh 0.5 mm, Fritsch mill D-55743, Germany) before hydrolysis to guarantee homogenous fibre digestion. In addition, key hydrolysis parameters were tested, and different conditions of centrifugation and washing steps, filtration, and neutralisation were applied.

2.4. Nanocellulose (CNC) characterization

2.4.1. Birefringence and haze

Well-known optical properties of CNC suspensions were used to detect a significant presence of CNC nanoparticles in isolated samples. To assess whether there was self-assembly of nanocrystals in suspension and films, the samples were observed in between crossed polarizers with a background source of light. For suspensions, this was done after shaking and standing for 5' to observe flow birefringence. The presence of this refractive property under shear indicated a biphasic behaviour (isotropic and nematic liquid crystal phases of CNC). If samples display permanent birefringence (no flow, at rest), the samples were considered to be in the chiral nematic regime (Habibi et al., 2010). The presence of haziness in dried films was also used for identification of chiral nematic phase formation.

2.4.2. Atomic force microscopy (AFM)

Atomic force microscopy (AFM) was performed to determine the morphology and dimensions of the isolated and commercial CNC by using a Ntrega Prima NT-MDT scanning probe microscope (Moscow, Russia). Before the observations, a few drops of diluted aqueous suspension (mildly ultrasonicated) were placed on a Si wafer and allowed to dry for 20' at RT. The samples were scanned in tapping mode, using ETALON probes, at RT. The length and width of CNC were measured using Nova Px software by manually obtaining the values from at least three different pictures, of which 20 values were averaged.

2.4.3. Fourier transform infrared spectroscopy (FTIR)

The surface chemistry of CNC were analysed by Fourier Transform InfraRed spectroscopy (FTIR) spectra. The samples were ground and mixed with KBr at a ratio of 1:100 (w/w) and pressed into thin pellets before analysis. A FTIR spectrometer (Nicolet 6700 from Thermo Fisher Inc., USA) was used from 400 to 4000 cm^{-1} at a resolution of 2 cm^{-1}. The acquired spectrum was an average of 32 scans.

2.4.4. X-ray diffraction (XRD)

XRD was performed on CNC with a Bruker D8 Advance diffractometer in Bragg-Brentano geometry ($\lambda = 1.78897$ Å), with lynxeye position sensitive detector. A cobalt tube with iron filter scattered from 5° to 55° while the sample was spinning, using step size 0.05° and counting time 0.8 s per step. The crystallinity index (CrI) was estimated according to the equation:

$$CrI(\%) = (I_{200} - I_{am}) / I_{200} \times 100$$

where I_{200} is referred to the maximum intensity of the 200 lattice diffraction peak at region around $2\theta = 26.1°$ and I_{am} is the intensity of diffraction for the amorphous part at around $2\theta = 21.0°$ (Segal et al., 1959). The angle values were translated from Cu Kα values to Co-equivalent by using Bragg's equation and d-spacing values for native cellulose (Poletto et al., 2014).

2.4.5. Bio-nanocomposites for mechanical performance

Bio-nanocomposites were made by adding the isolated and commercial CNC to Na-Alginate polymer matrix. CNC from TP and influent solids were chosen as a reference for the wastewater-recovered material. Sodium Alginate (mannuronate/guluronate = 1.56, Mw = 150 kg mol^{-1}) was obtained from Sigma-Aldrich, and was used as received. Thin-films were prepared by mixing equal parts of 2 wt% CNC suspensions with alginate solutions (2 wt%). The CNC volume fraction used was 50 vol% (density of both materials can be assumed as 1.5 g cm^{-3}). All mixtures were ultrasonicated for 5 min on ice prior and after mixing (Brandson ultrasonicator, 40% duty cycle, microtip limit 3). No remaining agglomerates were visible. The resulting dispersions were dried (20 °C, 50% RH) in a Petri dish. The storage modulus of dried Na-Alginate-CNC films was assessed by Dynamic Mechanical Analysis (DMA, PerkinElmer Pyris Series DMA7e, USA)) using rectangular strips (around 0.25 mm × 10 mm × 85 μm) cut out from the films. Testing was done in the linear regime for 2 min using tensile clamps at 1 Hz and 2 mm amplitude. The reinforcement efficiency (RE) was obtained by:

$$RE = (E_c - E_m) / E_m$$

where E_c is the modulus of composite and E_m is the modulus of matrix.

3. Results and discussion

3.1. Cellulose extraction

For the sieved influent solids, standard cellulose extraction procedure, with two NaOH extraction steps and one bleaching step, was sufficient to remove sludge and most of the colour (Fig. 2). Moreover, heating with demi water already eliminated some turbidity, and a layer of scum was formed, indicating fat removal. On the other hand, for Nereda® excess sludge, after first alkaline treatment (2 wt% NaOH), the samples were still viscous, and fibres presented a dark-brownish appearance. This was solved with more successive alkaline treatments - two times or more depending on wastewater solids characteristics - or even treatments with increased NaOH concentration (4–8 wt%). In general, after three consecutive alkaline treatments with NaOH, the resulting pulp was similar to the pulp obtained from influent solids. Without these steps, the samples always caused clogging during sieving, even with 350 μm sieves. Overall, following the NaOH treatments, a gradual decolouration of the sample occurred, leaving mainly cellulosic fibres. Non-cellulosic coloured material are well known to be partially solubilized in high alkaline conditions (dos Santos et al., 2016). This explains the high colour removal efficiency at high pH (13). The procedure is similar to what is applied in the delignification and pulping used by the paper industry to remove as much as possible the non-cellulosic components, i.e., hemicellulose and lignin-like compounds (García et al., 2016).

The number of bleaching steps varied per wastewater solid

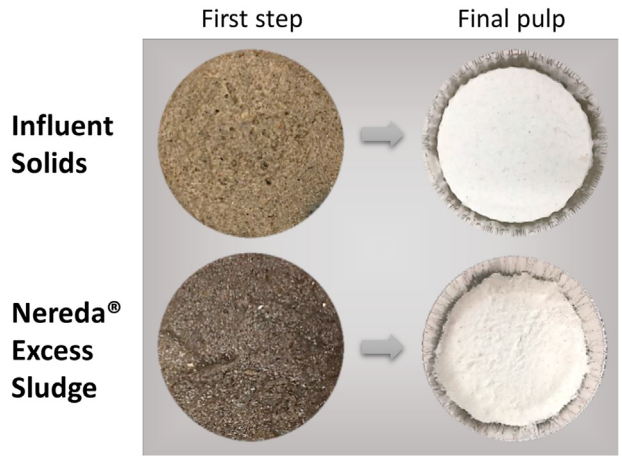

Fig. 2. The residues collected on sieve after the first cellulose extraction step and the final pulp for sieved influent solids (upper scheme), and Nereda® excess sludge (lower scheme).

investigated. For fibrous material that has been in contact with wastewater/sludge for a short time, such as influent solids, one bleaching step was sufficient to extract cellulose. The resulting fibres had a white appearance, which indicates low impurity (Fig. 2). The bleaching needed for excess sludge also varied between the samples collected. For sludge samples from the Nereda® plant, one bleaching step was sufficient. The bleaching of cellulose is performed for obtaining a more homogeneous and decolorized pulp (dos Santos et al., 2016). The slightly acidic chlorite (ClO^{2-}) bleaching can be performed in single or multiple steps, depending on the cellulose source, without considerably altering the intrinsic cellulose percentage of the sample. However, this procedure is not ideal due to the formation of bleaching by-products. Other more eco-friendly (but maybe less efficient) bleaching methods, such as the use of ozone, hydrogen peroxide, and, more recently, oxygen delignification with bleach effluent recovery could be explored in future (dos Santos et al., 2016; García et al., 2016).

Depending on the wastewater source, a lot of other inert debris can be present that interfere in the extraction and measurement of cellulose. Thus, it is imperative that, for cellulose quantification, the analysis is only carried out on wastewater/sludge where the cellulose input is much higher than that of other inert solids, such as sands, plastics, and seeds. This is a limitation of the proposed method. Moreover, dry milling at 0.5 mm mesh size has also resulted in some purification of the extracted pulp via fractionation. Heavier material deposit first, and the low-density (loosened) cellulose fibres remain on top, thus, can be separated.

With a defined method, the cellulosic content of wastewater samples could be determined, which can be found in Table 1. The cellulose of the influent solids was high, around 65% (g $g^{-1}_{dry\ matter}$). Excess sludge from the Nereda® reactor contained only 13–15% (g g^{-1}_{TSS}). The cellulosic content in wastewater solids can be interfered by varying human activity, seasonal changes, and pre-treatment (Ghasimi et al., 2015b).

As confirmed by the Van Soest method, both wastewater derived pulps showed a high cellulosic content (>86%), and low hemicellulose and lignin values (Table 2). In addition, a similar cellulose content, around 80%, was obtained for the reference toilet paper with both the developed and Van Soest methods (Tables 1 and 2). This validates the proposed cellulose extraction. Nevertheless, the Van Soest method as an approach for measuring the cellulose content of wastewater samples should be used with caution, since polysaccharides, proteins, and divalent cations can affect the assay (Chai and Udén, 1998). The limitations of this method are also related to its impracticality and the fact that at least 10 g of dry solids are required for the experiment. In this sense, the newly developed alkaline-bleaching method is a useful alternative.

3.2. Nanocellulose (CNC) isolation

Controlled acid hydrolysis was tested for CNC isolation from reference (microcrystalline cellulose, toilet paper) and recovered cellulosic pulp. The procedure varied per cellulose source, as hydrolysis conditions are crucial for obtaining the nanocrystals (Börjesson and Westman, 2015). For microcrystalline cellulose, reaction times were higher (>100 min), but all other conditions used were standard. Moreover, for microcrystalline cellulose, a direct strong acid addition (96.5%) on wet cellulose resulted in good CNC isolation, in agreement with Bondeson et al. (2006). Microcrystalline cellulose has a highly crystalline structure composed of bundles of heterogeneous cellulose microfibril aggregates, which are strongly hydrogen-bonded (dos Santos et al., 2016). Thus, microcrystalline cellulose is intrinsically harder to hydrolyse. In contrast, slightly higher cellulose to acid ratio (1:30 or 1:55) and shorter reaction times (45–60 min) were better for the isolation of CNC from toilet paper and recovered cellulose. The addition of cold 60% acid instead of 96.5% was also imperative. These settings avoided fast cellulose degradation and often resulted in a deep yellow reaction mixture after hydrolysis (colour reflects release of residual impurities, e.g. lignin). An increase in temperature from 45 to 50 °C also induced faster kinetics.

Toilet paper was also studied for regular and longer reaction times (60′ and 120′ reaction time, respectively). The longest reaction time resulted in a dark hydrolysis liqueur, where yellow-brownish impurities were formed. This indicates over-hydrolysis of the cellulose, with by-products formation (polymers, sugars, salts) (Reid et al., 2017; Silvério et al., 2013). More specifically, caramelization has happened (formation of C double bonds due to dehydration). For such samples, longer centrifugation-washing and dialysis cycles were necessary.

However, part of the colour developed during hydrolysis remained in all isolated CNC (Fig. 3), possibly because large sugars attached to the surface.

The CNC extraction procedure can include several post-treatment steps, such as washing, centrifugation, sonication, homogenization, dialysis, neutralisation. For the CNC isolated from microcrystalline cellulose and toilet paper, neutralisation with NaOH was required due to inefficient dialysis, which could have

Table 1
The yield of cellulosic pulp on initial dry mass and back-calculated concentrations for toilet paper and wastewater solids.

Sample	Cellulosic pulp (wt.% on initial dry matter)	Cellulose concentration (g Kg^{-1})
Toilet Paper	84.7	n.d.
Influent solids	64.8 ± 6.6	105.1 ± 5.3
Nereda® excess sludge 1	13.1 ± 0.4	10.1 ± 0.3
Nereda® excess sludge 2	15.3 ± 1.3	11.0 ± 0.9

n.d., not determined.

Table 2
Van Soest analysis for toilet paper and extracted cellulosic pulp.

Sample	Cellulose (wt.%)	Hemicellulose (wt.%)	Lignin (wt.%)
Toilet Paper[a]	80.3	9.2	4.2
Influent solids pulp	87.4	4.2	0.8
Nereda® excess sludge pulp	86.1	4.9	1.1

[a] Sample was analysed as is, and might contain additives.

caused adhesion of hydrolysis by-products on the nanocrystals (Reid et al., 2017). Neutralisation was also performed in previous studies by using 0.1–0.25 mM NaOH (Chen et al., 2016; Reid et al., 2017). Due to impurities of the wastewater-derived pulp, several centrifugation-washing cycles and filtration steps were also required to obtain CNC from influent solids and excess sludge cellulose. These impurities were still present in these pulp samples and were visible again at the bottom of the reaction flask after hydrolysis. Therefore, there is room for optimization in the rCNC production.

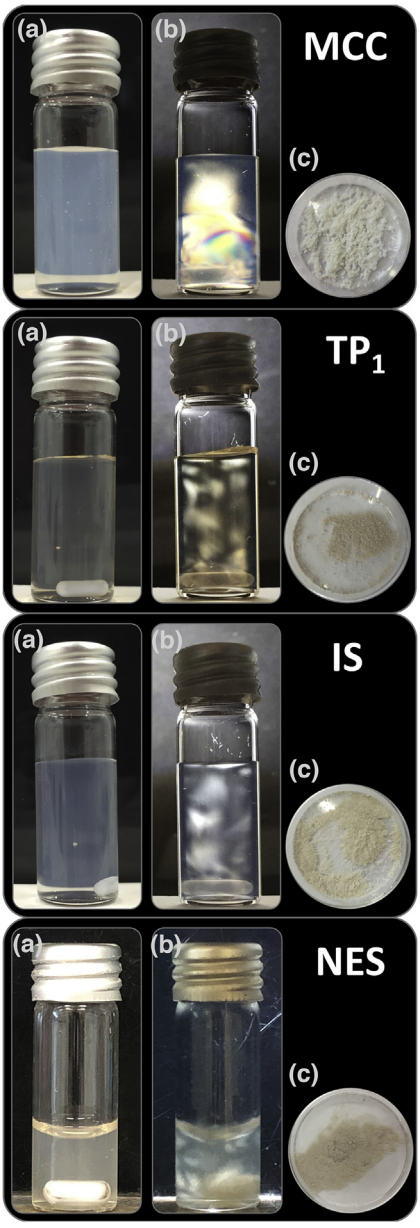

Fig. 3. Suspensions of CNC isolated from different sources: microcrystalline cellulose (MCC), toilet paper with regular extraction time (TP_1), sieved influent solids (IS), and Nereda® excess sludge (NES). Concentrations are ~1 wt% for MCC, and ~0.15 wt% for TP_1, IS, and NES. (a) Under normal illumination. (b) Under cross polarisation and shear. (c) Freeze-dried CNC powder.

The yields of (r)CNC on a pulp basis were 38%, 32.8%, 33.4 ± 17.9%, and 26.5 ± 8.2% for microcrystalline cellulose, toilet paper (60' reaction time), influent solids, and excess sludge pulps, respectively. This corresponds to 38%, 26.2%, 21.7 ± 11.6%, and 4 ± 1.2% (r)CNC per g source. The yield of CNC from microcrystalline cellulose is in accordance with literature (30%) (Bondeson et al., 2006). For toilet paper CNC and rCNC, the yield on an extracted-pulp basis was similar, but with large variation for the latter. Hydrolysis conditions, especially the reaction time, strongly influence the yield of (r)CNC, reflecting a balance between the cleavage of fibre amorphous domains and by-product formation. The CNC yields based on starting material mostly agree with values previously reported for waste paper (1.5–64%) and lignocellulosic wastes (26–77%) (García et al., 2016; Kumar et al., 2020; Silvério et al., 2013).

3.3. Nanocellulose (CNC) characterization

After obtaining suitable CNC isolation for each cellulose source, the visual appearance was compared. In aqueous suspensions of lab-made CNC, haze and dynamic birefringent domains were observed (Fig. 3), which is typical of CNC. In addition, a bluish-colour was observed for the CNC suspensions obtained from microcrystalline cellulose and influent solids. This bluish colour has also been reported for many types of CNC suspensions (Börjesson and Westman, 2015).

Chiral nematic CNC can reflect/transmit visible light depending on the length of the chiral pitch, where different wavelengths are reflected differently, and white light gets reflected emitting different colours. The chiral liquid crystal birefringence was more intense with higher CNC concentration in suspension and longer ultrasonication periods (dispersion of nanocrystals), as can be observed for the MCC sample. In very dilute regimes (<0.15 wt%), the suspensions did not show haziness nor birefringence (Figure A2, Text S4, Supporting information). In addition, the isolated CNC showed good colloidal stability in water (Figure A3, Text S5, Supporting information). The stability in water of the isolated-CNC can be attributed to negative hydroxyl groups from the cellulose structure and sulphate half esters groups grafted on the surface of nanocrystals during hydrolysis (Rajinipriya et al., 2018). This structure also assists in the formation of liquid crystal phases and affects the CNC rheology. Finally, thin flakes were produced via freeze-drying (Fig. 3), with an appearance similar to commercial products.

The isolated-(r)CNC samples show a rod-like morphology, similar in appearance to commercial CNC, as observed with AFM (Fig. 4). The nanocrystals length and diameter could also be estimated, and a relatively high aspect ratio (L/D: 10–14) was observed for the isolated (r)CNC. This aspect ratio was in line with the commercial CNC sample, which had an L/D of 15. Typical CNC aspect ratios range from 1 to 100 (Börjesson and Westman, 2015;

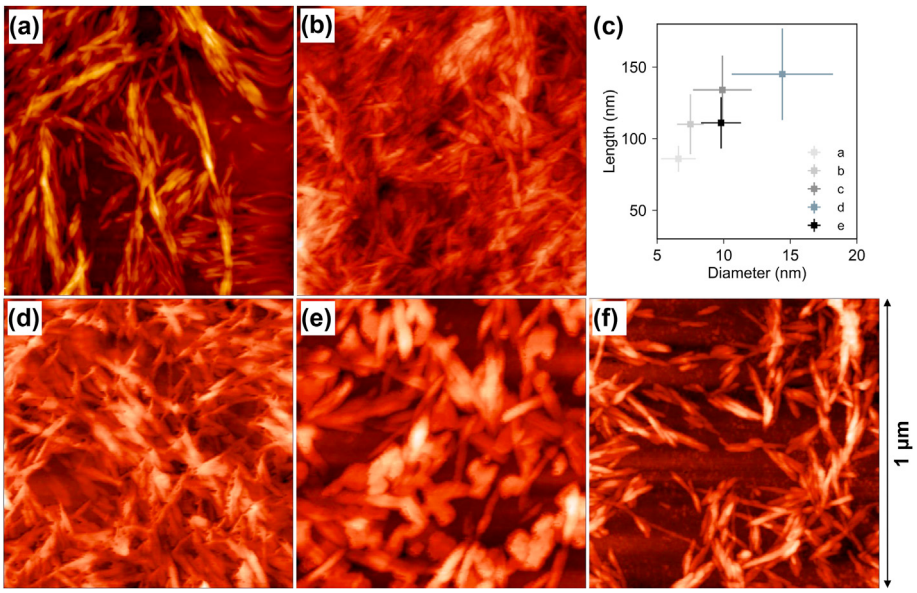

Fig. 4. AFM images of CNC from different sources: (a) commercial and isolated from (b) microcrystalline cellulose, (d) toilet paper with regular extraction time, (e) influent solids and (f) Nereda® excess sludge. The area covered by the images is 1 × 1 µm. (c) The diameter and length of the CNC samples is shown.

Reid et al., 2017). The average dimensions of CNC from microcrystalline cellulose and commercial CNC were in the same range, around 86–110 nm long and 7 nm wide. Interestingly, the (r)CNC isolated from toilet paper and wastewater-pulp had similar dimensions: lengths ranging from 111 to 134 nm and diameters from 10 to 14 nm. In a previous report, nanorods showed typical dimensions of 5–20 nm in diameter and 100–500 nm in length for several waste-recovered CNC (García et al., 2016). The morphology and dimensions are usually related to the hydrolysis conditions, such as acid to fibre ratio and acid concentration, hydrolysis time, temperature, in which extreme conditions can lead to shorter nanoparticles and higher dispersibility (Reid et al., 2017; Wang et al., 2019).

FTIR spectra were obtained to assess changes in surface chemistry with cellulose and CNC isolation treatments. The spectra are shown in full and also with a focus on the fingerprint region, which is assigned to stretching vibrations in the 1800–700 cm^{-1} region (Fig. 5). Some of the peaks observed can be attributed respectively to 1640 cm^{-1}: O-H bending vibration of absorbed water, 1428 cm^{-1}: CH_2 symmetric bending, 1160 cm^{-1}: C-O-C asymmetric stretching of cellulose, 1100 cm^{-1}: β-glucosidic ether linkages (C-O-C) of the anydroglucopyranose ring, 810 cm^{-1}: sulphonation. Features representative of cellulose I at 1428, 1160, and 1110 cm^{-1} wavelengths (Chen et al., 2016) are present in all samples of nanocellulose. All the isolated CNC showed strong similarities to the FTIR spectrum for commercial CNC. At 3400 cm^{-1} region, there is wrinkling in the spectra of MCC, TP_2, and TP_1. This can be related to the hydrophilic tendency of nanowhiskers. Furthermore, the appearance of a peak at 810 cm^{-1} is due to sulphate half ester groups attached to the nanocrystals via esterification. It is estimated that by using 64% sulphuric acid, around 0.5–2% sulphate half esters will be added to the CNC's surface (Börjesson and Westman, 2015). The analysis supports that cellulose and nanocellulose have been produced from wastewater solids.

The diffraction peaks of the studied CNC, see Fig. 6a, showed reflection peaks at 16.8°, 18.6°, 26.1°, and 40.4°, for all samples. These peaks are related to the crystal planes 110, 110, 200, and 040, respectively, which are commonly attributed to native cellulose I (Poletto et al., 2014). The major peak at 26.1° corresponds to the crystalline structure of cellulose I. These cellulose reflections are expected but also indicate that the primary crystal structure of the cellulosic source is preserved. The diffraction patterns of

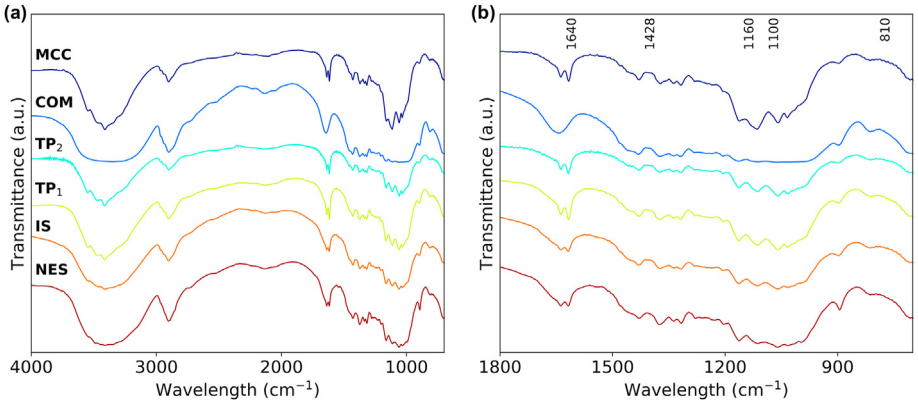

Fig. 5. FTIR spectra of CNC from microcrystalline cellulose (MCC), commercial CNC (COM), toilet paper with long (TP_2) and regular extraction time (TP_1), sieved influent solids (IS), Nereda® excess sludge (NES) origin (top-down curves respectively). (a) Full-length spectra with a highlight in the fingerprint region. (b) Zoomed view of fingerprint region.

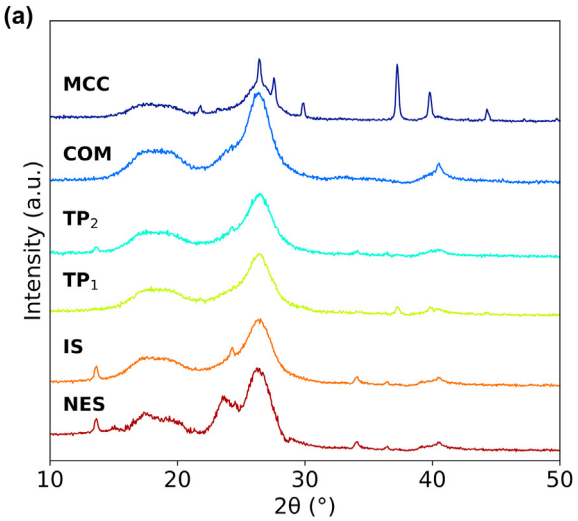

(b)

	CrI (%)
MCC	80
COM	73
TP_2	66
TP_1	65
IS	62
NES	68

Fig. 6. (a) X-ray diffractograms of CNC from microcrystalline cellulose (MCC), commercial CNC (COM), toilet paper with long (TP_2) and regular extraction time (TP_1), sieved influent solids (IS), Nereda® excess sludge (NES) origin (top-down curves respectively), with evidence on the peak's correspondent to the crystal lattice structure of native cellulose. (b) Crystallinity index of the samples obtained by the equation proposed by Segal et al.

wastewater-extracted rCNC are similar to commercial CNC. However, for wastewater-rCNC, other extra peaks were observed at 13.6°, 23.7°, and 34°. CNC from microcrystalline cellulose also showed many other peaks, with a major peak at 37.2°. They are resulting from the mineralisation of compounds from the acid hydrolysis or neutralisation steps, like Na_2SO_4. Based on the diffraction peak 200 and the amorphous region, the crystallinity index of samples could be estimated (Fig. 6b). CrI was similar among samples, ranging from 62 to 68% for toilet paper-based CNC. Overall, CrI for toilet paper-based sources is comparable to the value of commercial CNC (73%). Moreover, the crystallite size of CNC samples can also be estimated by using Scherrer's equation (Das et al., 2009). The crystallite values ranged from 4 to 8 nm for all the isolated-CNC and had an average size of 4.6 nm for the toilet paper-based CNC. This is in accordance with previously reported for cellulose (5 nm) (Poletto et al., 2014). This value represents a relative estimation of the crystalline portions of the isolated nanostructures, and is complementary to AFM dimensions. It is important to note that cellulose crystallites also present imperfections and, thus, a significant portion of the nanocellulose edges can still be less ordered or amorphous.

Bio-nanocomposites were produced with Na-Alginate and CNC of both commercial and lab origin (Fig. 7a). The films were opaque but translucent. In between polarizers, all films of Alginate-50 vol% CNC displayed a few birefringent domains, typical of the chiral nematic phase of CNC. The storage modulus for the produced films is shown in Fig. 7b. The modulus of a neat Na-Alginate film was 12 GPa, which by addition of 50 vol% commercial CNC increased to 19 GPa, resulting in the reinforcement efficiency of 58% for this filler. All isolated CNC increased the stiffness of alginate films to a similar value. The CNC from influent solids reinforced the modulus of alginate by 50% (18 GPa). The other isolated CNC (microcrystalline cellulose, TP) showed a relative increase in the alginate modulus of 42% and 83% (or 17 and 22 GPa), respectively. This is on par with the stiffness obtained using commercial CNC. The development of nanocellulose-reinforced composites takes advantage of the CNC's intrinsically high mechanical properties, aspect ratio, and surface area. In many studies, dramatic changes to the modulus of bio-nanocomposites are reported even at low CNC fraction (dos Santos et al., 2016; Wang et al., 2019). CNC have been used as a filler to reinforce composites with several biopolymers, such as cellulose acetate butyrate, chitosan, starch, and polylactic acid (Börjesson and Westman, 2015; Wang et al., 2019). Both optical and mechanical properties support the fact that the isolated toilet paper and wastewater-CNC have great potential as nanoparticle reinforcement agents.

Thus, the aspect ratio, morphology, chemical structure, crystallinity, and reinforcement of toilet paper-based CNC were convincingly similar to commercial CNC.

3.4. Nanocellulose from wastewater

The global production of household and sanitary paper (including toilet paper) was 36 million tons in 2018 (FAO, 2018). In the Netherlands only, it was estimated that toilet paper consumption is around 1 kg per person per month (Ruiken et al., 2013), which can amount to over 200 kt annually. Cellulosic wastewater solids (e.g., influent solids or excess sludge) are mostly being incinerated, digested, or composted, increasing the costs of waste management facilities. Alternatively, other uses have already been proposed, such as a soil conditioner, substrate for bioenergy, chemicals, construction material, composites, etc. (Da Ros et al., 2020; Ghasimi et al., 2016; Palmieri et al., 2019; Zhou et al., 2019). The origin of such waste is still the main limitation for reuse opportunities due to its appearance and odour. The alkaline-bleaching method for extracting pulp from wastewater recovers high-quality cellulose. Hence, it could be applied for developing (sustainable) recovered cellulose applications. Instead of using the raw recovered matter, resource recovery could shift towards the production of high-end materials, including nanocellulose.

Secondary sources of cellulose, such as waste paper, have not been suggested for CNC production until recently (Hietala et al., 2018; Kumar et al., 2020). The cellulose fraction in agro-wastes is usually lower than in waste paper, with cellulose varying from 25% (olive husks) to 56.5% (sunflower shells) and lignin values as high as 50.4% (García et al., 2016). Influent solids therefore showed to be a more attractive source for CNC production, with only a few pulping and bleaching steps required. This makes it an interesting source for CNC production due to its high cellulose content and abundance at a potentially low economical and energy cost. Nevertheless, other properties of wastewater-rCNC require research, such as thermal stability, charge density, etc.

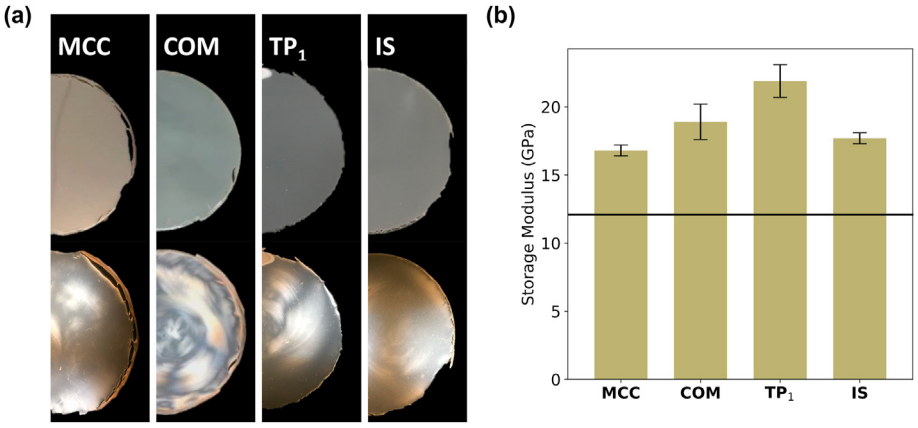

Fig. 7. (a) Alginate bio-nanocomposites with 50 vol% CNC from microcrystalline cellulose (MCC), commercial CNC (COM), Toilet paper (regular extraction time, TP_1), and sieved influent solids (IS) origin. Upper films are shown under normal illumination, whereas lower images are under cross polarisation. (b) Storage modulus of the bio-nanocomposites of Na-Alginate and CNC (50 vol%). The modulus of Na-alginate is indicated by the black horizontal line.

The nanocellulose from wastewater could also be investigated by studying alternative pre-treatments and isolation techniques. The latter can be chemical, by using other acid forms, oxidative and ionic liquid reaction, mechanical, or even microbial (Rajinipriya et al., 2018; Wang et al., 2019). Greener and more efficient methods could be found. For instance, Cellulose NanoFibres could be obtained with no chemicals required (Nechyporchuk et al., 2016). Therefore, implementing cellulose recovery aligned to nanocellulose production can be considered as an option. Nanocellulose recovery could even be done by means of a smart waste management with concomitant production of high-value products.

Finally, recovered nanocellulose shows potential for making fully wastewater-based bio-nanocomposites in combination with extracellular polymers extracted from excess sludges (Kaumera Nereda® Gum[1]) (Felz et al., 2016; Leeuwen, 2018). The need for alkaline conditions in both cellulose recovery and e.g. Kaumera® production gives options to integrate the recovery of both materials in a wastewater resource recovery facility. Nanocellulose composites have shown great mechanical and thermal properties while maintaining light transmittance and biodegradability (Wang et al., 2019). Bio-composites from wastewater-rCNC, possibly even in combination with other recovered materials, could result in novel and sustainable high-performance materials. Hence, the production of nanocellulose serves as an inspiring example of resource valorisation for the water sector in the broader context of a circular economy. For further information, the reader is referred to a public video (TU Delft TV/TU Delft, 2019).

4. Conclusions

A facile procedure for cellulose extraction and the determination of cellulose content in wastewater solids or sludge was demonstrated. The method is based on alkaline and bleaching treatments and, therefore, is source-specific. The studied sample only needs initial screening, however a cross-check by using the Van Soest method is recommended. This study covers extractions for sieved influent solids and excess sludge wastes, which can yield pulp with high cellulose fractions (>86 wt%).

Controlled acid hydrolysis can be used to isolate Cellulose NanoCrystals from toilet paper and wastewater derived cellulose. Wastewater-rCNC isolation is a feasible process since the yield based on cellulosic pulp can be above 30%. Sieved influent forms an attractive cellulose source with a high overall yield rCNC (22% g g_{solids}^{-1}) compared to Nereda® excess sludge (4% g g_{sludge}^{-1}). All the suspensions of CNC show visible flow birefringence, typical of this material. The TP- and wastewater-CNC are rod-like, around 130 nm long and 10 nm wide (L/D ratio ranges from 10 to 14). The functional groups on CNC are mainly correlated to the cellulose origin and severity of the acid treatment. The rCNC's crystallinity is comparable to that of commercial (62–68%). In addition, bio-nanocomposites of wastewater-CNC and Na-alginate can be produced via solvent-casting. It appears that wastewater-CNC is an attractive nanofiller, resulting in high stiffness bio-nanocomposites (18–22 GPa). The relative increment in stiffness by TP or wastewater-CNC addition ranges between 50 and 83%. This increment is remarkably similar to the commercial product (58%). Therefore, the aspect ratio, morphology, chemical structure, crystallinity, and reinforcement of wastewater-CNC samples are convincingly similar to the current commercial standard.

CRediT author statement

The authors share contributions to all the diverse steps involved in the published work.

Declaration of competing interest

The authors declare that they have no known competing financial interests or personal relationships that could have appeared to influence the work reported in this paper.

Acknowledgments

The authors are thankful to European centre of excellence for sustainable water technology (Wetsus) for financial support to the first author education. This work was financed by the Netherlands Organisation for Scientific Research (NWO), Earth and Life Sciences Division [grant number ALWGK.2016.025]. Authors are also grateful for the support by employees of Waternet (Chris Reijken), Royal HaskoningDHV, and of STPs Garmerwolde and Utrecht. CelluForce is acknowledged for supplying the commercial CNC: CelluForce NCC®. Ben Norder's assistance with DMA and XRD measurements is acknowledged. Marcel Bus's assistance with AFM is acknowledged. Thanks to Puck Merceij, Gijs Walstra, and Rosa Hendrikx for the journalistic video over this study.

[1] Kaumera Nereda® Gum mainly consists of the polymeric substances, i.e. glycoproteins, extracted from aerobic granular sludge. Kaumera® was formerly known as alginate-like exopolymers due to similar properties with alginate biopolymers.

Appendix A. Supplementary data

Supplementary data to this article can be found online at https://doi.org/10.1016/j.jclepro.2020.124507.

References

Ali, M., Wang, Z., Salam, K.W., Hari, A.R., Pronk, M., Van Loosdrecht, M.C.M., Saikaly, P.E., 2019. Importance of species sorting and immigration on the bacterial assembly of different-sized aggregates in a full-scale Aerobic granular sludge plant. Environ. Sci. Technol. https://doi.org/10.1021/acs.est.8b07303.

APHA, 1998. APHA: standard methods for the examination of water and wastewater. Am. Public Heal. Assoc. Water Work. Assoc. Environ. Fed. 552.

Bondeson, D., Mathew, A., Oksman, K., 2006. Optimization of the isolation of nanocrystals from microcrystalline cellulose by acid hydrolysis. Cellulose 13, 171–180. https://doi.org/10.1007/s10570-006-9061-4.

Börjesson, M., Westman, G., 2015. Crystalline nanocellulose — preparation, modification, and properties. Cellulose - Fundamental Aspects and Current Trends. https://doi.org/10.5772/61899.

Chai, W., Udén, P., 1998. An alternative oven method combined with different detergent strengths in the analysis of neutral detergent fibre. Anim. Feed Sci. Technol. 74, 281–288. https://doi.org/10.1016/S0377-8401(98)00187-4.

Charreau, H., Cavallo, E., Foresti, M.L., 2020. Patents involving nanocellulose: analysis of their evolution since 2010. Carbohydr. Polym. 237, 116039 https://doi.org/10.1016/j.carbpol.2020.116039.

Chen, R., Nie, Y., Kato, H., Wu, J., Utashiro, T., Lu, J., Yue, S., Jiang, H., Zhang, L., Li, Y.Y., 2017. Methanogenic degradation of toilet-paper cellulose upon sewage treatment in an anaerobic membrane bioreactor at room temperature. Bioresour. Technol. 228, 69–76. https://doi.org/10.1016/j.biortech.2016.12.089.

Chen, Y.W., Lee, H.V., Juan, J.C., Phang, S.M., 2016. Production of new cellulose nanomaterial from red algae marine biomass Gelidium elegans. Carbohydr. Polym. 151, 1210–1219. https://doi.org/10.1016/j.carbpol.2016.06.083.

Da Ros, C., Conca, V., Eusebi, A.L., Frison, N., Fatone, F., 2020. Sieving of municipal wastewater and recovery of bio-based volatile fatty acids at pilot scale. Water Res. https://doi.org/10.1016/j.watres.2020.115633.

Das, K., Ray, D., Bandyopadhyay, N.R., Ghosh, T., Mohanty, A.K., Misra, M., 2009. A study of the mechanical, thermal and morphological properties of microcrystalline cellulose particles prepared from cotton slivers using different acid concentrations. Cellulose 16, 783–793. https://doi.org/10.1007/s10570-009-9280-6.

dos Santos, F.A., Iulianelli, G.C.V., Tavares, M.I.B., 2016. The use of cellulose nanofillers in obtaining polymer nanocomposites: properties, processing, and applications. Mater. Sci. Appl. 7, 257–294. https://doi.org/10.4236/msa.2016.75026.

FAO, 2018. FAOSTAT Forestry Production and Trade [WWW Document]. FAO Yearb. http://www.fao.org/faostat/en/#data/FO. (Accessed April 2020).

Felz, S., Al-Zuhairy, S., Aarstad, O.A., van Loosdrecht, M.C.M., Lin, Y.M., 2016. Extraction of structural extracellular polymeric substances from aerobic granular sludge. JoVE, e54534. https://doi.org/10.3791/54534.

García, A., Gandini, A., Labidi, J., Belgacem, N., Bras, J., 2016. Industrial and crop wastes: a new source for nanocellulose biorefinery. Ind. Crop. Prod. 93, 26–38. https://doi.org/10.1016/j.indcrop.2016.06.004.

Ghasimi, D.S.M., de Kreuk, M., Maeng, S.K., Zandvoort, M.H., van Lier, J.B., 2016. High-rate thermophilic bio-methanation of the fine sieved fraction from Dutch municipal raw sewage: cost-effective potentials for on-site energy recovery. Appl. Energy 165, 569–582. https://doi.org/10.1016/j.apenergy.2015.12.065.

Ghasimi, D.S.M., Tao, Y., de Kreuk, M., Abbas, B., Zandvoort, M.H., van Lier, J.B., 2015a. Digester performance and microbial community changes in thermophilic and mesophilic sequencing batch reactors fed with the fine sieved fraction of municipal sewage. Water Res. 87, 483–493. https://doi.org/10.1016/j.watres.2015.04.027.

Ghasimi, D.S.M., Tao, Y., De Kreuk, M., Zandvoort, M.H., Van Lier, J.B., 2015b. Microbial population dynamics during long-term sludge adaptation of thermophilic and mesophilic sequencing batch digesters treating sewage fine sieved fraction at varying organic loading rates. Biotechnol. Biofuels 8, 171. https://doi.org/10.1186/s13068-015-0355-3.

Giesen, A., de Bruin, L.M.M., Niermans, R.P., van der Roest, H.F., 2013. Advancements in the application of aerobic granular biomass technology for sustainable treatment of wastewater. Water Pract. Technol. 8, 47–54. https://doi.org/10.2166/wpt.2013.007.

Habibi, Y., Lucia, L.A., Rojas, O.J., 2010. Cellulose nanocrystals: chemistry, self-assembly, and applications. Chem. Rev. 110, 3479–3500. https://doi.org/10.1021/cr900339w.

Hietala, M., Varrio, K., Berglund, L., Soini, J., Oksman, K., 2018. Potential of municipal solid waste paper as raw material for production of cellulose nanofibres. Waste Manag. 80, 319–326. https://doi.org/10.1016/j.wasman.2018.09.033.

Jordan, J.H., Easson, M.W., Dien, B., Thompson, S., Condon, B.D., 2019. Extraction and characterization of nanocellulose crystals from cotton gin motes and cotton gin waste. Cellulose 26, 5959–5979. https://doi.org/10.1007/s10570-019-02533-7.

Klemm, D., Kramer, F., Moritz, S., Lindström, T., Ankerfors, M., Gray, D., Dorris, A., 2011. Nanocelluloses: a new family of nature-based materials. Angew. Chem. Int. Ed. 50, 5438–5466. https://doi.org/10.1002/anie.201001273.

Kumar, V., Pathak, P., Bhardwaj, N.K., 2020. Waste paper: an underutilized but promising source for nanocellulose mining. Waste Manag. 102, 281–303. https://doi.org/10.1016/j.wasman.2019.10.041.

Leeuwen, K. Van, 2018. The energy & raw materials Factory : role and potential contribution to the circular economy of The Netherlands. Environ. Manage. 786–795. https://doi.org/10.1007/s00267-018-0995-8.

Mabrouk, A. Ben, Dufresne, A., Boufi, S., 2020. Cellulose nanocrystal as ecofriendly stabilizer for emulsion polymerization and its application for waterborne adhesive. Carbohydr. Polym. 229 https://doi.org/10.1016/j.carbpol.2019.115504.

Nechyporchuk, O., Belgacem, M.N., Bras, J., 2016. Production of cellulose nanofibrils: a review of recent advances. Ind. Crop. Prod. 93, 2–25. https://doi.org/10.1016/j.indcrop.2016.02.016.

Nussbaum, B.L., Soros, A., Mroz, A., Rusten, B., 2014. Removal of particulate and organic matter from municipal and industrial wastewaters using fine mesh rotating belt sieves. Proc. Water Environ. Fed 2006, 3052–3056. https://doi.org/10.2175/193864706783750907.

Palmieri, S., Cipolletta, G., Pastore, C., Giosuè, C., Akyol, Ç., Eusebi, A.L., Frison, N., Tittarelli, F., Fatone, F., 2019. Pilot scale cellulose recovery from sewage sludge and reuse in building and construction material. Waste Manag. https://doi.org/10.1016/j.wasman.2019.09.015.

Paulsrud, B., Rusten, B., Aas, B., 2014. Increasing the sludge energy potential of wastewater treatment plants by introducing fine mesh sieves for primary treatment. Water Sci. Technol. 69, 560–565. https://doi.org/10.2166/wst.2013.737.

Poletto, M., Ornaghi Júnior, H.L., Zattera, A.J., 2014. Native cellulose: structure, characterization and thermal properties. Materials 7, 6105–6119. https://doi.org/10.3390/ma7096105.

Pronk, M., 2016. Aerobic Granular Sludge: Effect of Substrate on Granule Formation. PhD Thesis. Delft University of Technology.

Pronk, M., de Kreuk, M.K., de Bruin, B., Kamminga, P., Kleerebezem, R., van Loosdrecht, M.C.M., 2015. Full scale performance of the aerobic granular sludge process for sewage treatment. Water Res. 84, 207–217. https://doi.org/10.1016/j.watres.2015.07.011.

Qin, L., Gao, H., Xiong, S., Jia, Y., Ren, L., 2020. Preparation of collagen/cellulose nanocrystals composite films and their potential applications in corneal repair. J. Mater. Sci. Mater. Med. 31 https://doi.org/10.1007/s10856-020-06386-6.

Rajinipriya, M., Nagalakshmaiah, M., Robert, M., Elkoun, S., 2018. Importance of agricultural and industrial waste in the field of nanocellulose and recent industrial developments of wood based nanocellulose: a review. ACS Sustain. Chem. Eng. 6, 2807–2828. https://doi.org/10.1021/acssuschemeng.7b03437.

Reid, M.S., Villalobos, M., Cranston, E.D., 2017. Benchmarking cellulose nanocrystals: from the laboratory to industrial production. Langmuir 33, 1583–1598. https://doi.org/10.1021/acs.langmuir.6b03765.

Reijken, C., Giorgi, S., Hurkmans, C., Pérez, J., van Loosdrecht, M.C.M., 2018. Incorporating the influent cellulose fraction in activated sludge modelling. Water Res. https://doi.org/10.1016/j.watres.2018.07.013.

Roy, S., Zhai, L., Van Hai, L., Kim, J.W., Park, J.H., Kim, H.C., Kim, J., 2018. One-step nanocellulose coating converts tissue paper into an efficient separation membrane. Cellulose 25, 4871–4886. https://doi.org/10.1007/s10570-018-1945-6.

Ruiken, C.J., Breuer, G., Klaversma, E., Santiago, T., van Loosdrecht, M.C.M., 2013. Sieving wastewater - cellulose recovery, economic and energy evaluation. Water Res. 47, 43–48. https://doi.org/10.1016/j.watres.2012.08.023.

Rusten, B., Odegaard, H., 2006. Evaluation and testing of fine mesh sieve technologies for primary treatment of municipal wastewater. Water Sci. Technol. 54, 31–38. https://doi.org/10.2166/wst.2006.710.

Segal, L., Creely, J.J., Martin, A.E., Conrad, C.M., 1959. An empirical method for estimating the degree of crystallinity of native cellulose using the X-ray diffractometer. Textil. Res. J. 29, 786–794. https://doi.org/10.1177/004051755902901003.

Shun'ichi, K.H., Naoyuki, M., Iwahori, Honda, S., Miyata, N., Iwahori, K., 2002. Recovery of biomass cellulose from waste sewage sludge. J. Mater. Cycles Waste Manag. 4, 46–50. https://doi.org/10.1007/s10163-001-0054-y.

Silvério, H.A., Flauzino Neto, W.P., Pasquini, D., 2013. Effect of incorporating cellulose nanocrystals from corncob on the tensile, thermal and barrier properties of poly(vinyl alcohol) nanocomposites. J. Nanomater. https://doi.org/10.1155/2013/289641.

Trache, D., Thakur, V.K., Boukherroub, R., 2020. Cellulose nanocrystals/graphene hybrids—a promising new class of materials for advanced applications. Nanomaterials 10, 1523. https://doi.org/10.3390/nano10081523.

TU Delft TV/TU Delft, 2019. The Hidden Gems of Wastewater. YouTube: youtu.be/cC0-LYWHoXg. (The Netherlands). (Accessed April 2020).

Van Soest, P.J., Wine, R.H., 1967. Use of detergents in the analysis of fibrous feeds. IV. Determination of plant cell-wall constituents. JAOAC (J. Assoc. Off. Anal. Chem.) 50, 50–55. https://doi.org/10.1016/j.ijhydene.2012.08.110.

Wang, J., Liu, X., Jin, T., He, H., Liu, L., 2019. Preparation of nanocellulose and its potential in reinforced composites: a review. J. Biomater. Sci. Polym. Ed. 30, 919–946. https://doi.org/10.1080/09205063.2019.1612726.

Zhou, Y., Stanchev, P., Katsou, E., Awad, S., Fan, M., 2019. A circular economy use of recovered sludge cellulose in wood plastic composite production: recycling and eco-efficiency assessment. Waste Manag. https://doi.org/10.1016/j.wasman.2019.08.037.